COBEM 2021 26th International Congress of Mechanical Engineering
November 22-26, 2021, Virtual Congress, Brazil

Interactions Between small-friction Particles in Very Narrow Solid-Liquid Fluidized Beds

Vinícius Pereira da Silva Oliveira
Fernando David Cúñez Benalcázar
Nicolao Cerqueira Lima
Erick de Moraes Franklin
School of Mechanical Engineering - University of Campinas, Rua Mendeleyev, 200, Campinas - SP, CEP: 13083-860, Brazil
viniciuspereirasilv@gmail.com, david.cunez@hotmail.com, nicolaol@hotmail.com, franklin@fem.unicamp.br

Abstract. *Granular systems have various applications in industry and possess an important role in the development of novel technologies in transport and processing of grains. A particular case of these systems are fluidized beds, that are described as suspensions of solid particles (grains) in a vertical duct by an ascendant fluid flow forced against a porous plate. The bed behavior and characteristics are influenced by the interstitial fluid. When considering a liquid or for low particle concentrations, fluid interactions such as drag, buoyancy and virtual mass are dominant; if the fluid is a gas, particle interactions like shocks and solid friction prevail. When those beds have a size ratio of 10 or less between tube and grain diameters, it is said that is a very narrow fluidized bed. Narrow fluidized beds have very rich dynamics both at the bed (macroscopic) and the grain (microscopic) scales, with crystallization, blockages and formation of plugs occurring at the bed scale, and shocks, sliding and vortex shedding at the grain scale. In this work we investigate how the properties of grains influence very narrow solid-liquid fluidized beds. We focus on understanding the role of friction between grains and between the grains and the wall, including the absence of friction in very narrow solid-liquid fluidized beds. We analyze their behavior at the macroscopic scales and its trajectories. The results show that the average bed height increases with the friction coefficient, but the mobility of individual particles decreases.*

Keywords: *Fluidized bed, small-friction, plug regime, crystallization*

1. INTRODUCTION

Granular systems have various applications in industry and possess an important role in the development of novel technologies, in transport and processing of grains. In the particular case of fluidized beds, due to its high mass and heat transfers and simple construction, they are frequently applied in combustion or gaseification of coal and biomass (Cúñez and Franklin, 2019, 2020b). Fluidized beds can be described as suspensions of solid particles (grains) in a vertical duct by an ascendant fluid flow forced against a porous plate, in which the flow rate is sufficient to generate enough drag force to balance or surpass its net weight (Guazzelli, 2004).

Although of its simple setup, fluidized beds have a very rich dynamics and are full of heterogeneities both at the bed (macroscopic) and the grain (microscopic) scales, being susceptible to different regimes and flow patterns (Guazzelli, 2004; Cúñez and Franklin, 2020a). Its dynamics comprehends particle-particle, particle-fluid and particle-wall interactions. The interstitial fluid also has an influence on the bed regime, where liquids or low concentration of particles make the fluid interactions dominant, such as drag, buoyancy and virtual mass; or, on the other hand, with gases, particle interactions like shocks and solid friction are more active (Cúñez and Franklin, 2020a; Cúñez *et al.*, 2021). Other phenomenona like crystallization, blockages and formation of plugs can also be observed in fluidized beds. They are usually a consequence of the small ratio between the particle size and the bed diameter, where very narrow fluidized beds can be defined as those where this ratio is approximately 10 or less (Cúñez and Franklin, 2019). Cúñez and Franklin (2019) investigated the dynamics of granular plugs in water fluidized beds in narrow tubes experimentally and numerically. They observed the formation of granular plugs that propagate upward and measured its characteristic lengths and celerities. Their results show that the length of plugs strongly depended on the water flow and are independent of the initial height of the bed, but bed celerities varies with both the initial bed height and water flow.

Despite all the works developed to describe interparticle and particle-wall collisions, few of them focused specifically at the influence of particle-particle friction factor on the bed dynamics. Joseph *et al.* (2001) made experimental measurement at the approach and rebound of a particle colliding with a wall in a viscous fluid and found that the coefficient of restitution increases with increasing Stokes number beyond a certain critical value, but experiments did not consider the friction factor. Later, Joseph and Hunt (2004) performed a more comprehensive study with the approach and rebound of different smoothness particles in a smooth wall in a viscous fluid and proposed a model considering the coefficient of restitution, rotational coefficient of restitution and sliding friction factor. they also observed that in smooth particles, the

lubrication effects result in a reduction in sliding friction factor by an order of magnitude. Aguilar-Corona *et al.* (2011) investigated collisions inside a liquid fluidized bed experimentally and made measurements of coefficient of restitution and collisional frequency. They found that the evolution of coefficient of restitution as a function of the Stokes number, based on the normal impact velocity agree well with experimental data of Joseph *et al.* (2001) and Joseph and Hunt (2004), but the results are limited to friction coefficients lesser than 0.025.

In this work, we focus on the investigation on how the friction coefficient influences very narrow solid-liquid fluidized beds. We present experiment and numerical simulation analyses at macroscopic scale and grain motion, and evaluate the effect of the variation of the friction coefficient on the bed dynamics.

2. METHODOLOGY

2.1 Experimental Setup

The experiments were conducted in a water circuit filmed by a CMOS (complementary metal oxide semiconductor) camera. This circuit consists in a heat exchanger (that ensures a stable flow temperature of 25 ± 3 ºC), a water tank, an inlet line, a pump (with a maximum capacity of 4100 l/h), a flow meter, a flow homogeneizer (consisting of a 150 mm long polymethylmetacrylate - PMMA - filled with alumina beads of 6 mm diameter to ensure uniform flow at the inlet of the section test), a 25.4 mm diameter tube of polymethylmetaclylate and an outlet line. A sketch of the experimental setup is presented at the Fig. 1.

The species tested in this work were white polymer beads with low friction applications (commercial airsoft BBs bullets) with 6 mm diameter. Measurements showed that the weight is between $0.2 \pm 0.005g$ ($\rho = 1768.38 \pm 44.21$ kg/m^3, which is superior to the water's specific mass, $\rho = 1000$ kg/m^3). Beads are showed in Fig. 2. The tested beds consisted of $N = 300$ particles, with cross sectional velocity of 0.110 m/s applied to the bed at experiments. The terminal velocity v^*, Reynolds number Re^* and terminal Stokes Number St^* calculated by correlations of Clift *et al.* (1978) are respectively 0.5936 m/s, 3548 and 698. Once the bed is placed in test section, a fluid flow is imposed in order to shuffle the bed and let the grains settle by free fall, then bed is fluidized.

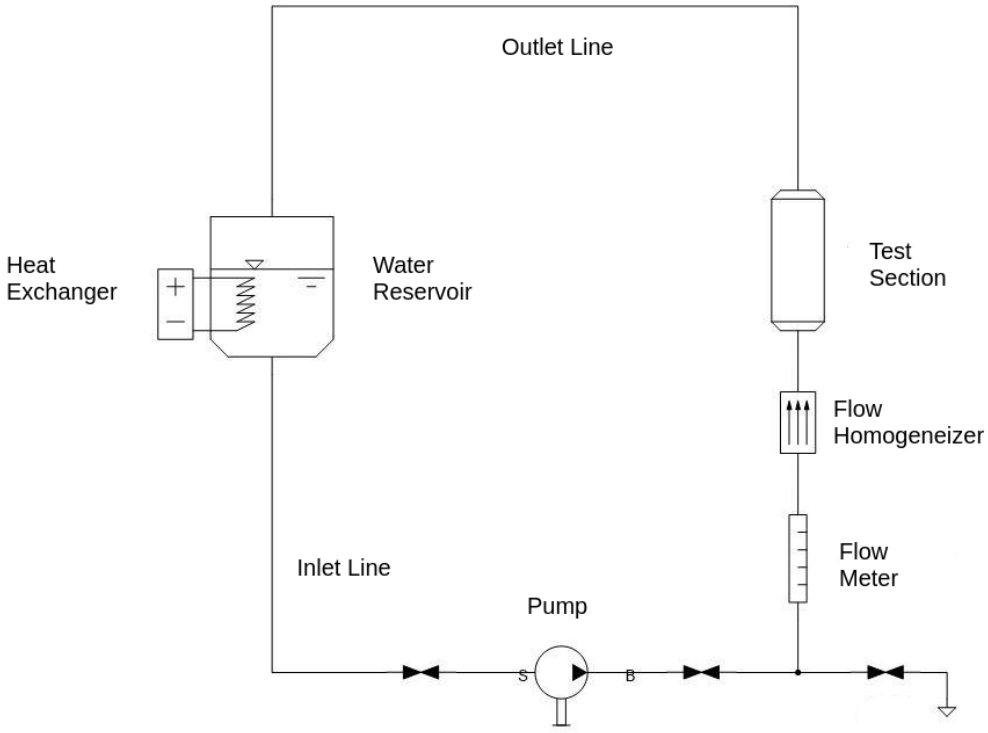

Figure 1. Scketch of the water circuit used in Experimental set.

Figure 2. Particles in packing bottle. Hexagonal lattice can be observed.

2.2 Numerical Setup

In our numerical simulations, we used the open source code CFDEM that couples OpenFoam, used to compute the fluid domain in a eulerian frame of reference with LIGGGHTS, to compute the grain dynamics in a lagrangian frame of reference. In fluidized bed simulations, where narrow pipes are considered, the particle diameter is usually larger than the cell size. Therefore, we made use of an unresolved method where the region of influence of the particles is artificially increased, and their volume is then compensated by adding a fictitious porosity.

On the DEM side, LIGGGHTS solves the linear and angular momentum equations, as shown in Eqs. (1) and (2). The fluid motion, on the other hand, is described by the incompressible volume-averaged Navier–Stokes equations, shown in Eqs. (3) and (4).

$$m_p \frac{d\mathbf{u_p}}{dt} = \mathbf{F_D} + \mathbf{F_{stress}} + \mathbf{F_{am}} + \mathbf{F_g} + \mathbf{F_c}, \tag{1}$$

$$I_p \frac{d\boldsymbol{\omega_p}}{dt} = \mathbf{T_c}, \tag{2}$$

$$\frac{\partial \rho_f \varepsilon_f}{\partial t} + \nabla \cdot (\rho_f \varepsilon_f \mathbf{u_f}) = 0, \tag{3}$$

$$\frac{\partial \rho_f \varepsilon_f \mathbf{u_f}}{\partial t} + \nabla \cdot (\rho_f \varepsilon_f \mathbf{u_f} \mathbf{u_f}) = -\varepsilon_f \nabla P + \varepsilon_f \nabla \cdot \boldsymbol{\tau_f} - \frac{\mathbf{F_D}}{V_{cell}}, \tag{4}$$

m_p is the particle mass, I_p is the particle inertia, $\mathbf{u_p}$ is the particle velocity, $\boldsymbol{\omega_p}$ is the particle angular velocity, $\mathbf{T_c}$ is the contact torque resultant between particles, $\mathbf{F_D}$ is the drag force of fluid on particles, $\mathbf{F_C}$ is the resultant contact force between two particles, $\mathbf{F_g}$ is the gravitational force, $\mathbf{F_{stress}}$ is the force caused by the fluid stress as described by Eq. 5, $\mathbf{F_{am}}$ is the added mass force and V_p is the particle volume. For fluid mass and momentum conservation, $\mathbf{u_f}$ is the fluid velocity, ε_f is fluid volume fraction, P is the pressure, $\boldsymbol{\tau_f}$ is the deviatoric stress tensor of the fluid and V_{cell} is the volume of the considered cell.

$$\mathbf{F_{stress}} = V_p[-\nabla P + \nabla \cdot \boldsymbol{\tau}], \tag{5}$$

Numerical simulations were set to have the same conditions as experiments, varying the friction factor. The particle properties are shown in Tab. 1. 0 value at interparticle friction generates error in simulations, then, a near 0 value was set to the friction factor. In all simulations, the wall-particle friction factor was neglected.

The problem is initialized by distributing the particles randomly in the domain and allowing them to settle by free fall. The superficial velocity is linearly increased, until it reaches the test superficial velocity at 0.8 s. The domain has cylindrical shape with 25.4 mm diameter with 0.6 m height. For the boundary conditions, a fixed velocity and zero pressure gradient was set at inlet, a fixed zero pressure and zero velocity gradient were set at outlet and a no-slip boundary condition at the wall. The total simulation time was 15 s.

Table 1. Simulated particle and fluid properties.

Particle diameter d	6 mm
Particle density ρ_p	1770 kg/m^3
Young Modulus E	3.0×10^9 Pa
Poisson ratio σ	0.21
Restitution coefficiente	0.5
Particle-particle friction coefficient μ_{pp}	0.001, 0.2, 0.4, 0.6, 0.8, 1.0
Particle-wall friction coefficient μ_{pw}	0.0
Liquid density ρ_f	1000 kg/m^3
Liquid viscosity μ_f	0.001 Pa.s

2.3 Image Processing

The image processing was made using C++, with OpenCV libraries and CodeBlocks IDE. The images were segmented from movies by a matlab script, then the source images are split in the HSV color space and the hue matrix information was processed, as it better segments the bed. The region of interest (ROI) is isolated, and holes in image are refined by a top-hat morphological operation. Once it is processed, the data from macroscopic structures are tracked, and plugs and void bubbles are detected by the particle phase in tube view plane (as it is a 2D plane, occluded particles are not detected). Stages of the processing can be seen in the Fig. 3. The length of tube in vertical image plane direction has the form of Eq. 6. So by a discrete sum, the void fraction in section has the form of Eq. 7.

$$l(x) = 2\sqrt{x(D-x)}, \tag{6}$$

$$\phi = \frac{\sum l(x_i)}{2\pi N^2} \tag{7}$$

where $l(x)$ is the length of the tube at the vertical direction of the plane of image, x is the horizontal coordinate, D is the tube diameter, ϕ is the particle fraction and N is the number of pixel alongside the tube diameter. $2\pi N$ refers to the area of the tube in square pixel.

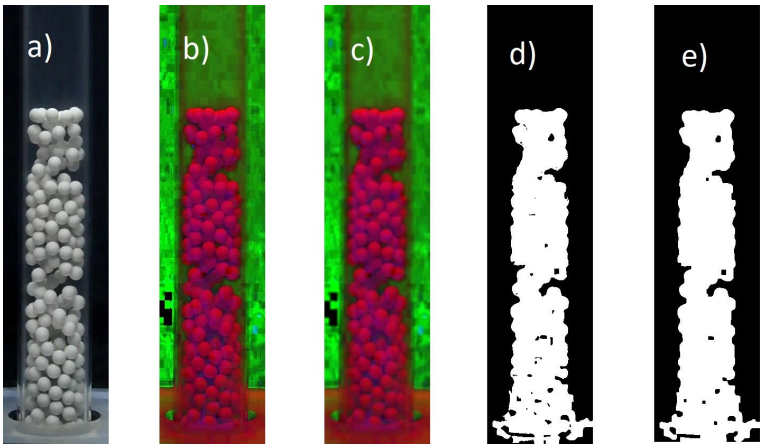

Figure 3. Results of image processing.

3. RESULTS

3.1 Macroscopic Analysis

In both experiments and simulations, plug regime was observed. Mean bed height $\bar{h}$ and spationtemporal diagram was made in order to analyze bed macroscopic phenomenona in which changes in interparticle friction factor affects in the bed scale. The simulation results for the mean bed height $\bar{h}$ considering different friction factors f are shown at Fig. 4. The red curve shows a linear adjust with minimum quadratic method. We can observe that the curve fits well the numerical data and shows a linear increase of the mean bed height with the increase of the friction factor.

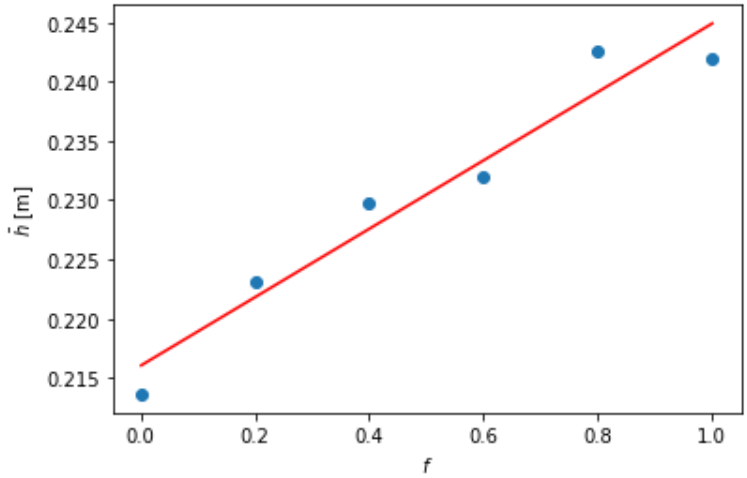

Figure 4. Average bed height versus friction factor from simulations.

The experiment with BBs given a mean bead height of 0.2264 m. Fig. 5 compares spatiotemporal diagram at the top of plugs in the simulation with $f = 0.2$ and the top of plugs in experiments. As the friction between the particles and the wall are neglected in the simulations it is expected that plugs have higher celerities than ones observed in experiments, due to the lack of interactions with the wall in the first. For different friction factors in simulations we can see that the inclination of position versus time of plugs are approximately the same. From that is possible to conclude that that interparticle friction factor does not affect the celerities of plugs.

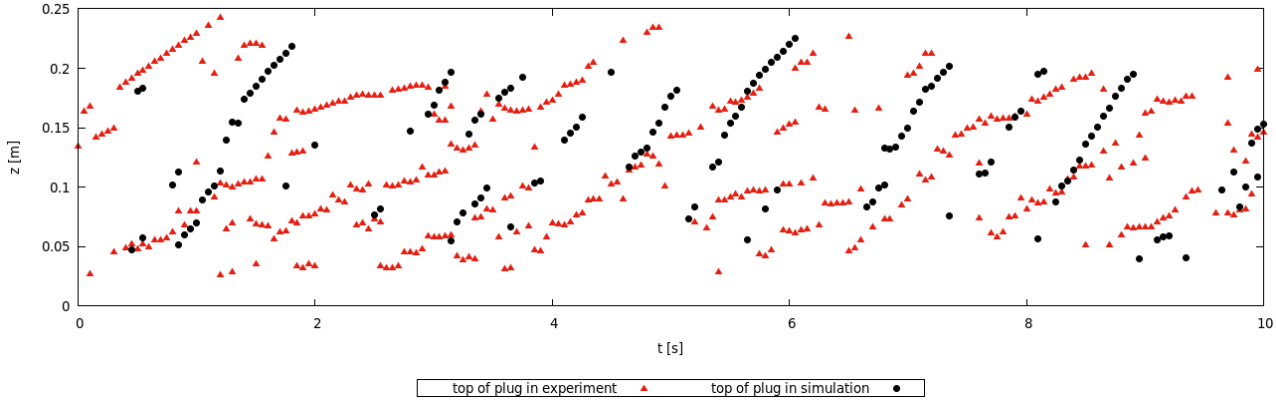

Figure 5. Comparison between spatiotemporal diagrams of experiment and the 0.2 interparticle friction factor simulation.

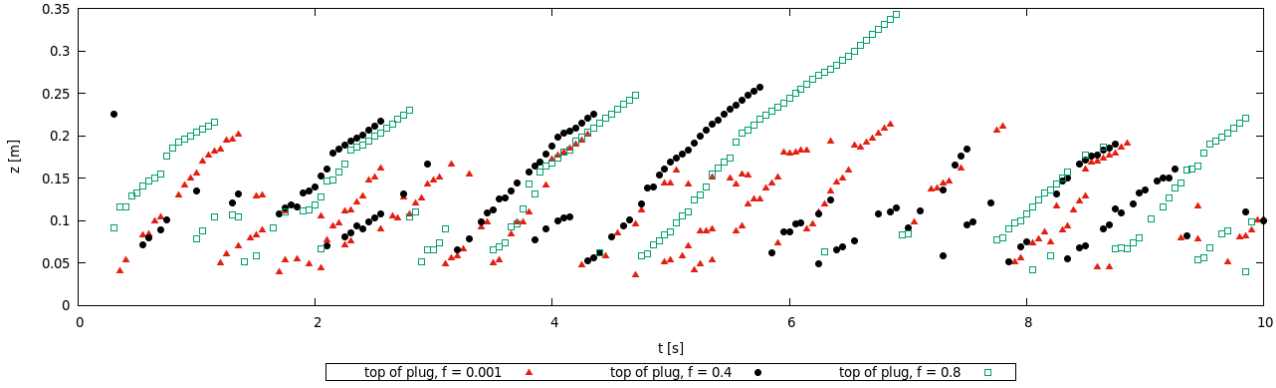

Figure 6. Crossed spatiotemporal diagrams showing the motion of the top of the plugs from simulations with different friction factors.

3.2 Microscopic Analysis

Particle trajectory was tracked for each simulation as particle position is available at each time-step. Results are shown in Fig. 7, it can be observed that the increase in friction factor reduced the mobility of particles along the z axis. The plots correspond to the same time span of 15 s and one particle was tracked in each case.

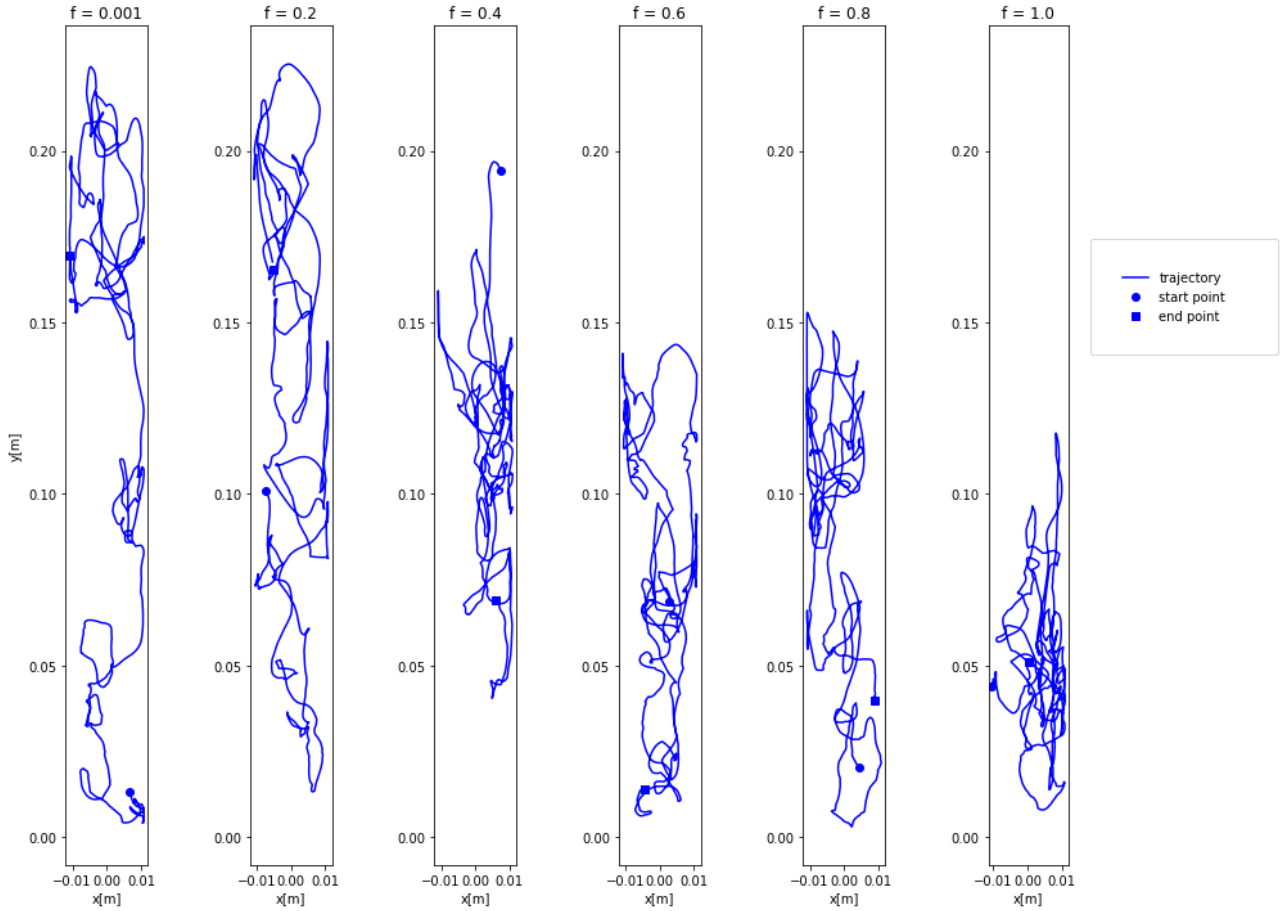

Figure 7. Different simulation trajectories from simulations.

4. CONCLUSIONS

In this work, we investigated the macroscopic behavior and trajectories of particles in a very narrow fluidized bed varying interparticle friciton factor, in order to observe how it influences phenomena at the bed. We recorded videos from experiments of a fluidized bed with airsoft BBs beads and made numerical simulations with the same conditions varying the interparticle friction factor. Then, we processed the images in order to acquire information of macroscopic structures and the grains motion, with an algorithm using OpenCV, and numeric data processing.

From the data acquired, we could observe that, as friction factor increases, the mean bed height also increases. A linear adjust is proposed to fit the data. Also, plug regime is observed and analyzing particle fraction in order to make spatiotemporal diagrams, it can be observed that plug celerities seems to be unchanged by changes in the friction factor. The plugs in numerical simulations presented higher celerities than experiments, which indicate the role of wall friction in plug celerities, as simulations have zero wall friction factor. Particle tracking shows more mobility along the z axis as the interparticle friction is reduced.

5. ACKNOWLEDGEMENTS

The authors are grateful to FAPESP (Grants numbers 2018/14981-7, 2016/18189-0, 2019/20888-2 and 2020/00211-0).

6. REFERENCES

Aguilar-Corona, A., Zenit, R. and Masbernat, O., 2011. “Collisions in a liquid fluidized bed”. *International Journal of Multiphase Flow*, Vol. 37, p. 695–705.

Clift, R., Grace, J.R. and Weber, M.E., 1978. *Spheres at High Reynolds Numbers*. Bubbles, Drops and Particles. Academic Press, INC.

Cúñez, F.D. and Franklin, E.M., 2019. "Plug regime in water fluidized beds in very narrow tubes". *Powder Technology*, Vol. 345, pp. 234–246.

Cúñez, F.D. and Franklin, E.M., 2020a. "Crystallization and jamming in narrow fluidized beds". *Physics of Fluids*, Vol. 32, p. 083303.

Cúñez, F.D. and Franklin, E.M., 2020b. "Mimicking layer inversion in solid-liquid fluidized beds in narrow tubes". *Powder Technology*, Vol. 364, No. 1, pp. 994–1008.

Cúñez, F.D., Lima, N.C. and Franklin, E.M., 2021. "Motion and clustering of bonded particles in narrow solid-liquid fluidized beds". *Physics of Fluids*, Vol. 33, p. 023303.

Guazzelli, E., 2004. *Fluidized Beds: From Waves to Bubbles*. The Physics of Granular Media. Wiley-VCH Verlag GmbH & Co. KGaA.

Joseph, G.G. and Hunt, M.L., 2004. "Oblique particle–wall collisions in a liquid". *Journal of Fluid Mechanics*, Vol. 510, p. 71–93.

Joseph, G.G., Zenit, R., Hunt, M.L. and Rosenwinkel, A.M., 2001. "Particle–wall collisions in a viscous fluid". *Journal of Fluid Mechanics*, Vol. 433, p. 329–346.

7. RESPONSIBILITY NOTICE

The authors are solely responsible for the printed material included in this paper.